Extremophiles (2012) 16:227–236
DOI 10.1007/s00792-011-0422-z

ORIGINAL PAPER

Identification of cold-inducible inner membrane proteins of the psychrotrophic bacterium, *Shewanella livingstonensis* Ac10, by proteomic analysis

Jungha Park · Jun Kawamoto · Nobuyoshi Esaki · Tatsuo Kurihara

Received: 27 July 2011 / Accepted: 13 December 2011 / Published online: 3 January 2012

Abstract *Shewanella livingstonensis* Ac10 is a psychrotrophic Gram-negative bacterium that grows at temperatures close to 0°C. Previous proteomic studies of this bacterium identified cold-inducible soluble proteins and outer membrane proteins that could possibly be involved in its cold adaptation (Kawamoto et al. in Extremophiles 11:819–826, 2007). In this study, we established a method for separating the inner and outer membranes by sucrose density gradient ultracentrifugation and performed proteomic studies of the inner membrane fraction. The cells were grown at temperatures of 4 and 18°C, and phospholipid-enriched inner membrane fractions were obtained. Two-dimensional polyacrylamide gel electrophoresis and peptide mass fingerprinting analysis of the proteins identified 14 cold-inducible proteins (more than a 2-fold increase at 4°C). Six of these proteins were predicted to be inner membrane proteins. Two predicted periplasmic proteins, 5 predicted cytoplasmic proteins, and 1 predicted outer membrane protein were also found in the inner membrane fraction, suggesting their association with the inner membrane proteins and/or lipids. These cold-inducible proteins included proteins that are presumed to be involved in chemotaxis (AtoS and PspA), membrane protein biogenesis (DegP, SurA, and FtsY), and morphogenesis (MreB). These findings provide a basis for further studies on the cold-adaptation mechanism of this bacterium.

Communicated by A. Driessen.

J. Park · J. Kawamoto · N. Esaki · T. Kurihara (✉)
Institute for Chemical Research, Kyoto University,
Uji, Kyoto 611-0011, Japan
e-mail: kurihara@scl.kyoto-u.ac.jp

Keywords Cold-adapted bacterium · Cold adaptation · Cold-inducible proteins · Inner membrane · Membrane proteins · Proteomics · *Shewanella livingstonensis*

Abbreviations

LB	Luria–Bertani
SDS-PAGE	Sodium dodecyl sulfate polyacrylamide gel electrophoresis
2DE	Two-dimensional gel electrophoresis
PMF	Peptide mass fingerprinting
SRP	Signal recognition particle

Introduction

Psychrophilic and psychrotrophic microorganisms have colonized permanently cold environments, such as the deep sea and Polar Regions. Recent studies revealed that these organisms have developed several strategies to cope with cold environments, including the production of cold-active enzymes (Feller and Gerday 2003; Siddiqui and Cavicchioli 2006), modulation of lipid composition to maintain the fluidity of the cell membrane (Russell 1997; Chintalapati et al. 2004), and the production of RNA chaperones to suppress the formation of undesired secondary structures of RNA (Yamanaka et al. 1998; Hebraud and Potier 1999). However, the molecular mechanisms responsible for cold adaptation in these microorganisms remain largely unknown, especially those localized in the cellular membranes.

We have been studying the bacterium *Shewanella livingstonensis* Ac10 as a model for the investigation of microbial cold-adaptation mechanisms. *S. livingstonensis*

Ac10 is a cold-adapted bacterium, isolated from Antarctic seawater, that grows well at temperatures close to 0°C but does not grow at temperatures above 30°C (Kulakova et al. 1999). It is a Gram-negative bacterium with a cell surface structure composed of three morphologically distinct layers: an inner membrane bordering the cytoplasm, a periplasm containing the peptidoglycan layer external to the inner membrane, and an outer membrane at the external surface of the cell (Murray et al. 1965). The inner and outer membranes differ both in composition and function. The outer membrane generally functions as a selective barrier that protects the bacteria from harmful compounds in the environment. The inner membrane proteins are involved in many key cellular processes such as energy generation and conversion in the respiratory chain, cell division, signal transduction, and transport processes. Previous proteomic analysis of *S. livingstonensis* Ac10 identified 26 soluble proteins and 2 outer membrane proteins that are inducibly expressed at a temperature of 4°C, whereas no cold-inducible inner membrane protein was identified (Kawamoto et al. 2007). Proteomic studies of other cold-adapted bacteria have also been carried out, but cold-inducible inner membrane proteins have not been analyzed comprehensively so far (Ting et al. 2010; Piette et al. 2011; Wilmes et al. 2011). Proteomic analysis of the inner membrane is often difficult due to the presence of a large amount of outer membrane proteins in the crude membrane fraction. Thus, it is desirable to separate inner and outer membranes to facilitate identification of inner membrane proteins. Moreover, actual subcellular localization cannot be determined without separation of the two membranes, because prediction of subcellular localization based on the primary protein structure does not consider protein–protein interactions and protein–lipid interactions that affect the localization of proteins.

In this study, we performed proteome analysis of the inner membrane proteins of *S. livingstonensis* Ac10. We established a method for separating the inner and outer membranes and successfully identified the inner membrane proteins that are inducibly expressed at low temperatures, thus providing a better understanding of the cold-adaptation mechanism of this bacterium.

Materials and methods

Bacterial strain and culture conditions

S. livingstonensis Ac10 that had been isolated from Antarctic seawater was grown in 5 ml of Luria–Bertani (LB) medium (pH 7.0) for 48 h at 18°C, and then transferred to 300 ml of LB medium for further cultivation at 4 and 18°C. We confirmed that the densities of viable cells at the end of the exponential phase are comparable at 4 and 18°C by cultivating the cells recovered at this point on LB medium, suggesting that cultivation at 18°C is not significantly deleterious to this bacterium compared with that at 4°C.

Preparation of the inner membrane fraction

The procedure for preparation of the inner membrane fraction was based on equilibrium density gradient centrifugation of the total membrane fraction, obtained by lysis of spheroplasts. Spheroplasts were prepared using a modified version of the method of Osborn and Munson (1974) and Yamato et al. (1975): The cells were grown as described above until the early stationary phase ($OD_{600} = 1.0$) and harvested by centrifugation. Cell pellets (approximate wet weight 1 g) were resuspended in 30 ml of ice-cold 0.75 M sucrose/10 mM Tris–HCl (pH 7.8), and 100 μg/ml lysozyme was added. Conversion to the spheroplast form was accomplished by dilution with ice-cold 1.5 mM EDTA (pH 8.0) to a total of 2 volumes of the original suspension. The spheroplasts were lysed by sonication, and intact cells and cellular debris were removed by 15 min of centrifugation at 1,600×*g*. Membranes were separated from the cytoplasmic fraction by 100 min of centrifugation at 226,240×*g* (L8-55; Beckman, Palo Alto, CA, USA). The membrane pellet was diluted with 9 ml of ice-cold solution containing 0.25 mM sucrose, 3.3 mM Tris–HCl (pH 7.8), and 1 mM EDTA and centrifuged for 100 min at 226,240×*g*. The washed membrane fraction was suspended in 2 ml of 25% sucrose (w/w)/5 mM EDTA (pH 7.5). Then, 1 ml of the crude membrane fraction was layered on 4 ml of 35–50% sucrose linear gradient (w/w) containing 5 mM EDTA (pH 7.5) in the centrifuge tubes of an SW 50.1 rotor (Beckman). The gradients were centrifuged for 16 h at 226,240×*g*, and 0.5 ml fractions were collected from the top of the tubes.

Lipid quantification

Phospholipids were extracted from an aliquot of each fraction by the method of Bligh and Dyer (Bligh and Dyer 1959). Total phospholipids were determined by quantifying the inorganic phosphate released from phospholipids, as described by Rouser et al. (1966) with slight modifications. In brief, 200 μl of 70% perchloric acid was added to each dried sample. After incubation at 200°C for 1.5 h, 1.4 ml of MilliQ water/2.5% ammonium molybdate/10% ascorbic acid (5:1:1; v/v/v) was added to the sample mixture, and the mixture was vortexed. Subsequently, 400 μl of MilliQ water was added, followed by another period of incubation at 100°C for 10 min. The absorbance at 820 nm was then measured. Potassium phosphate was used as a standard for quantification.

Proteome analysis

Proteins (300 μg) were loaded onto ReadyStrip™ IPG Strips, pH 3–10 (17 cm, Bio-Rad Laboratories Inc., Hercules, CA, USA), and isoelectric focusing was performed with PROTEAN IEF Cell (Bio-Rad Laboratories Inc.) as recommended by the manufacturer. In situ alkylation treatment of the gel strips for the second-dimensional sodium dodecyl sulfate polyacrylamide gel electrophoresis (SDS-PAGE) was carried out as described previously (Mineki et al. 2002), and SDS-PAGE was performed using the gel with 12.5% acrylamide. After fixation and staining with SYPRO Ruby (Invitrogen Corp., Carlsbad, CA, USA), the gels were scanned with an image analyzer (Typhoon 9400: GE Healthcare UK Ltd., Buckinghamshire, UK). The protein expression patterns were analyzed using the image analysis software PDQuest ver. 7.0 (Bio-Rad Laboratories Inc.). All values of spot intensities were normalized with the intensities of three proteins, TPR repeat-containing protein, FoF_1 ATP synthase beta subunit, and FKBP-type peptidyl-prolyl *cis–trans* isomerase, which were found in equal amounts in the two-dimensional gel electrophoresis (2DE) images of the crude membrane of the cells grown at 4°C (Fig. 1) and 18°C (data not shown). After scanning, the gels were restained with the Negative Gel Stain MS Kit (Wako Pure Chemical Industries Ltd., Osaka, Japan). Spots were excised from the 2DE gels, and the proteins were digested with sequencing-grade modified trypsin (Promega, Madison, WI, USA) for tryptic in-gel digestion. The tryptic digests were purified using ZipTip C18 (Millipore, Bedford, MA, USA) and a solution containing 80% acetonitrile (ACN) and 0.1% trifluoroacetic acid (TFA) for elution to ensure the collection of hydrophobic peptides. Peptide mass fingerprinting (PMF) analysis was performed using the standard method with Autoflex II MALDI-TOF MS systems (Bruker Daltonics, Billerica, MA, USA). Alpha-cyano-4-hydroxycinnamic acid (Bruker Daltonics) matrix (1 mg/ml in 90% ACN and 0.1% TFA) was used. Calibration was performed using the Peptide Calibration Standard (Bruker Daltonics). A local version of Mascot (Matrix Science Ltd., London, UK) and the whole genome sequence of *S. livingstonensis* Ac10 were used to identify the proteins. Mascot search was performed with tolerances of 150 ppm for the fragment ions assuming up to one missed cleavage. The data were searched with a fixed modification of a β-propionamide modification of cysteine and variable modifications of oxidation of methionine and phosphorylation of serine, threonine, and tyrosine. The threshold of the Mascot score was set at 50 for protein identification (Koenig et al. 2008). Automated predictions of the subcellular localization of bacterial proteins were made using the PSORT program (http://psort.hgc.jp/).

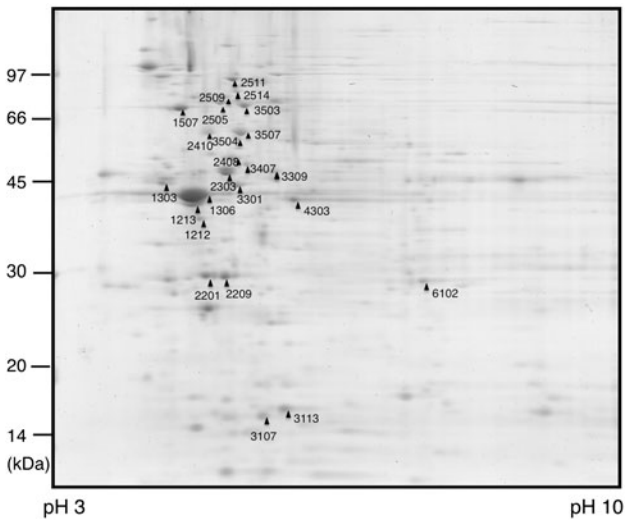

Fig. 1 Two-dimensional gel electrophoresis of crude membrane proteins from *S. livingstonensis* Ac10 grown at 4°C. The gel was stained with SYPRO Ruby, and peptide mass fingerprinting analysis was performed using the standard method with the Autoflex II MALDI-TOF MS system

Results

Proteome analysis of the crude membrane fraction prepared from the spheroplasts of *S. livingstonensis* Ac10

S. livingstonensis Ac10 was grown at a temperature of 4°C until the early stationary phase, and the crude membrane fraction was subjected to 2DE to identify the major membrane proteins. Figure 1 shows the gel image for the crude membrane fraction; 24 protein spots with high intensities (above 2,000 ppm) were excised from the gel and identified by PMF analysis with a sequence database of *S. livingstonensis* Ac10. The theoretical molecular weight and isoelectric point of the identified proteins matched well with those observed in the 2DE gels (Fig. 1; Table 1). The identified proteins included 12 predicted outer membrane proteins, 4 predicted inner membrane proteins, 2 predicted periplasmic proteins, and 6 predicted cytoplasmic proteins.

Separation of inner and outer membranes by sucrose density gradient ultracentrifugation

In the above experiment, a large proportion of the identified proteins were predicted to be outer membrane proteins, and only a small number of predicted inner membrane proteins were identified. Separating the inner and outer membranes facilitates the identification of inner membrane proteins, and subcellular fractionation enables their actual localization to be determined with greater accuracy than

Table 1 Crude membrane proteins of *S. livingstonensis* Ac10 grown at 4°C

Spot #	Gene	Protein[a]	Molecular mass (kDa)[b]	p*I*[b]	Predicted localization[c]	Accession no.
Group 1. Protein synthesis, folding, and translocation						
1213	*tpr*	TPR repeat-containing protein	46.7	9.23	IM	AB646433
2511	*yaeT*	Surface antigen D15	92.9	4.71	OM	AB646437
3503	*rpsA*	Ribosomal protein S1	61.2	4.81	CY	AB285527
6102	*pspA*	Phage shock protein A	25.6	6.80	IM	AB646434
3504	*tig*	FKBP-type peptidyl-prolyl *cis–trans* isomerase (trigger factors)	54.2	4.85	PE	AB284101
2509	*dnaK*	Chaperone protein DnaK	33.0	4.80	CY	AB284103
3507	*groL*	Chaperonin GroL	57.1	4.72	CY	AB646435
3113	*rpsF*	30S ribosomal protein S6	14.9	5.06	CY	AB646436
3309	*tufB*	GTPase-translation elongation factor	33.3	4.57	CY	AB284113
Group 2. Membrane transport						
4303	*ompA*	Outer membrane protein A	42.5	5.77	OM	AB284075
2514	*gspD*	General secretion pathway protein D	77.2	4.79	OM	AB646438
1212	*ompC*	Omp_C176	37.7	4.46	OM	AB284090
2209	*tsx2*	Nucleoside-specific channel-forming protein	32.0	4.81	OM	AB646439
3301	*tolC2*	Type I secretion outer membrane protein, TolC family protein	47.1	4.86	OM	AB373986
3407	*tolCl*	Outer membrane protein efflux pump	52.3	4.82	OM	AB284106
1303	*oppA*	Hypothetical protein	41.5	4.13	OM	AB284107
1306	*sliv_c417088*	Porin	44.7	4.35	OM	AB646440
2408	*atpD*	FoF_1 ATP synthase β subunit	49.9	4.67	IM	AB646451
2303	*sliv_c449084*	Phosphate-selective porin O and P	43.4	4.77	OM	AB646441
1507	*cirA*	TonB-dependent receptor	71.9	4.24	OM	AB373987
Group 3. Metabolism						
3107	*ribH*	Riboflavin synthase	101.9	8.37	CY	AB646475
Group 4. Motility						
2505	*pilQ*	Type IV pilus secretin PilQ	74.5	4.65	OM	AB646442
Group 5. Unknown function						
2201	*sliv_c028017*	Hypothetical protein	28.9	4.66	PE	AB646443
2410	*sliv_c361036*	Hypothetical protein	43.5	4.62	IM	AB646444

[a] Proteins in the database showing the highest sequence similarity to the proteins from *S. livingstonensis* Ac10

[b] Molecular mass and p*I* values were calculated using the draft genome sequence of *S. livingstonensis* Ac10

[c] Predicted localizations are characterized as follows: *OM* outer membrane, *PE* periplasm, *IM* inner membrane, *CY* cytoplasm

predictions based on primary structure, because the predictions do not consider protein–protein interactions and protein–lipid interactions, which may affect protein localization.

We performed sucrose density gradient ultracentrifugation of the crude membrane fraction to separate inner and outer membranes. The crude membrane fraction was prepared from cells grown at 4 and 18°C. Figure 2 shows the sucrose density and phospholipid content of each fraction obtained after ultracentrifugation. From the cells grown at 4 and 18°C, 10 and 25% of phospholipids, respectively, were obtained from the bottom fraction. In the middle fractions, (44–47% (w/w) sucrose for the cells grown at 4°C, and 41–44% (w/w) sucrose for the cells grown at 18°C), approximately 50% of the total phospholipids were recovered. The sucrose density of the phospholipid-enriched fraction from the cells grown at 4°C was higher than that for the cells grown at 18°C. proOmpA, a precursor of outer membrane protein OmpA, was found in the middle fractions but not in the bottom fractions, indicating that the inner membrane was enriched in the middle fractions (data not shown). Enrichment of the inner membrane in the middle fractions was further evidenced by identification of the proteins recovered in these fractions as described below.

Global identification of cold-inducible inner membrane proteins

As described above, we obtained phospholipid-enriched fractions in the middle of the sucrose density gradient. We

performed proteomic analysis of these fractions to determine whether the inner membrane was enriched in these fractions and to identify inner membrane proteins that are inducibly expressed at low temperatures, which might support cold adaptation of *S. livingstonensis* Ac10. The third fraction for cells grown at 4°C and the fifth fraction for cells grown at 18°C (Fig. 2) were analyzed by 2DE. The 2DE images for the phospholipid-enriched fractions obtained from the cells grown at 4 and 18°C showed 276 and 382 protein spots, respectively, with intensities above 500 ppm (Fig. 3a, b). About 100 spots that were visible by negative staining were excised from the gel for PMF analysis, and 52 proteins could be identified (Table 2), 19 of which were predicted inner membrane proteins; 6 were predicted outer membrane proteins; 22 were predicted cytoplasmic proteins; and 5 were predicted periplasmic proteins. The identified proteins were classified into the following six groups according to their sequence similarity to the proteins in the database (Table 2): protein synthesis, folding, and translocation (group 1); membrane transport (group 2); cell division and morphogenesis (group 3); metabolism (group 4); other functions (group 5); and unknown function (group 6). Fourteen of the proteins were cold-inducible (more than a 2-fold increase at 4°C). Six were predicted inner membrane proteins (AtoS, PspA, MreB, FtsY, Ald, and SdhA); 1 was a predicted outer membrane protein (Sliv_c417088); 2 were predicted periplasmic proteins (DegP and SurA); and 5 were predicted cytoplasmic proteins (Dpp4, PykF, LeuB, SucB, and RibP_PPkin). Proteins decreased at 4°C were also identified (Table 2).

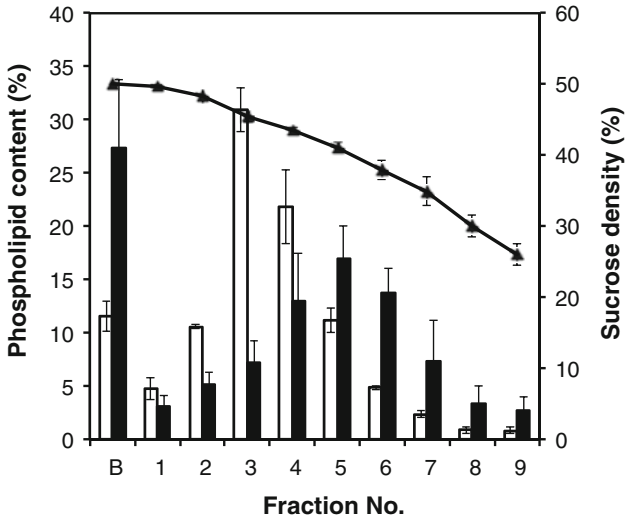

Fig. 2 Separation of inner and outer membranes of *S. livingstonensis* Ac10 by sucrose density gradient ultracentrifugation. Crude membranes from the cells grown at 4°C (*open bar*) and 18°C (*closed bar*) were subjected to sucrose density gradient ultracentrifugation. Experiments were performed four times for each sample. Phospholipids in each fraction were quantified by measuring inorganic phosphate (1–9). The pellets at the bottom of the sucrose density gradient tube were suspended with 500 µl of 5 mM EDTA (pH 7.5)/50% sucrose and used for phosphorus quantification (*B*). Means and standard deviations are indicated

Discussion

Separation of inner and outer membranes of *S. livingstonensis* Ac10 and identification of cold-inducible inner membrane proteins

In this study, we established a method for separation of the inner and outer membranes of *S. livingstonensis* Ac10 for efficient identification of inner membrane proteins. We performed sucrose density gradient ultracentrifugation of the crude membranes that were prepared from the cells

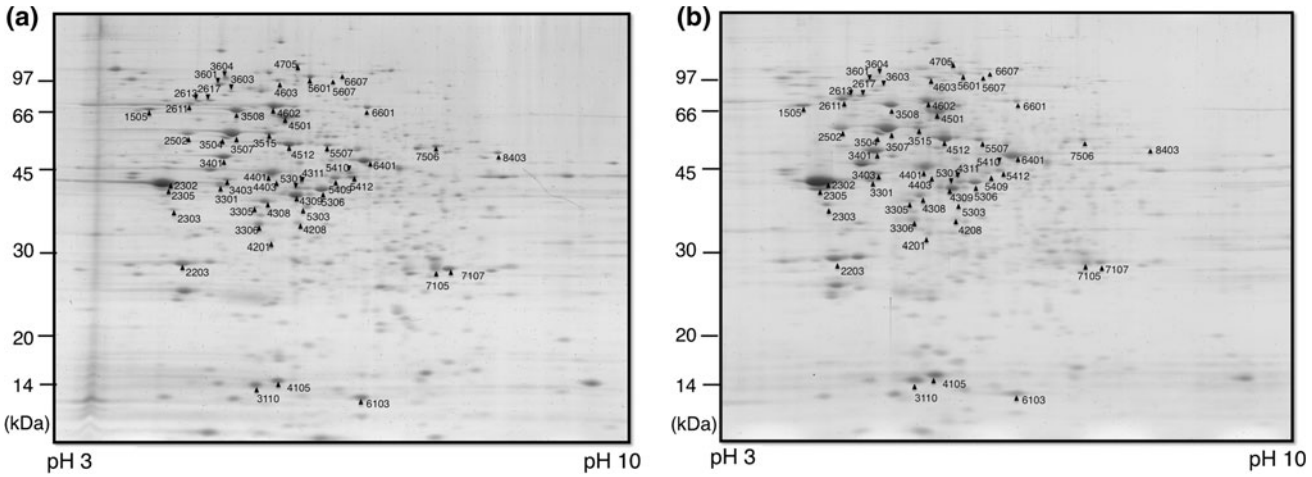

Fig. 3 Comparison of proteins in the inner membrane fractions from *S. livingstonensis* Ac10 grown at 4°C (**a**) and 18°C (**b**). The gels were stained with SYPRO Ruby and analyzed with PDQuest ver. 7.0

Table 2 Proteins in the inner membrane fractions of *S. livingstonensis* Ac10 grown at 4 and 18°C

Spot #	Gene	Protein[a]	Molecular mass (kDa)[b]	pI[b]	Spot intensity (ppm) 4°C/18°C	Relative abundance (4°C/18°C)	Predicted localization[c]	Accession no.
Group 1. Protein synthesis, folding, and translocation								
2305	*tpr*	TPR repeat-containing protein	46.7	9.23	4,584/7,119	0.64	IM	AB646433
3601	*yaeT*	Surface antigen D15	92.9	4.71	5,340/4,363	1.22	OM	AB646437
4201	*tsf*	Translation elongation factor Ts	30.2	5.05	1,971/2,916	0.68	CY	AB646445
5409	*degP*	Protease Do	47.1	6.02	7,391/1,898	3.89	PE	AB646446
3508	*rpsA*	Ribosomal protein S1	61.2	4.81	15,518/11,205	1.38	CY	AB285527
7107	*pspA*	Phage shock protein A	25.6	6.80	14,425/6,408	2.25	IM	AB646434
6607	*dpp4*	Peptidase S9 prolyl oligopeptidase	104.1	5.77	4,465/869	5.14	CY	AB646447
2611[d]	*surA*	PpiC-type peptidyl-prolyl *cis–trans* isomerase	68.4	4.49	5,992/6,803	0.88	PE	AB648914
2613[d]	*surA*	PpiC-type peptidyl-prolyl *cis–trans* isomerase	68.4	4.49	3,610/1,719	2.10	PE	AB648914
3504	*tig*	FKBP-type peptidyl-prolyl *cis–trans* isomerase (trigger factors)	54.2	4.85	4,300/4,848	0.89	PE	AB284101
2617	*dnaK*	Chaperone protein DnaK	33.0	4.80	2,998/3,214	0.93	CY	AB284103
3507	*groL*	Chaperonin GroL	57.1	4.72	4,684/20,516	0.23	CY	AB646435
6103	*rplI*	50S ribosomal protein L9	15.5	5.99	19,501/11,860	1.64	CY	AB646448
4105	*rpsF*	30S ribosomal protein S6	14.9	5.06	15,900/18,268	0.87	CY	AB646436
4401	*tufB*	GTPase-translation elongation factor	33.3	4.57	22,044/16,844	1.31	CY	AB284113
Group 2. Membrane transport								
4309	*ompA*	Outer membrane protein A	42.5	5.77	21,365/11,895	1.79	OM	AB284075
2303	*ompC*	Omp_C176	37.7	4.46	3,614/4,850	0.75	OM	AB284090
4603	*epsE*	Polysaccharide export protein	96.7	5.15	4,279/2,691	1.59	IM	AB646449
3403	*tolC2*	Type I secretion outer membrane protein, TolC family protein	47.1	4.86	5,077/5,461	0.94	OM	AB373986
6601	*tat*	Twin-arginine translocation pathway signal	83.2	7.49	4,798/3,795	1.26	IM	AB646450
2302	*sliv_c417088*	Porin	44.7	4.35	95,923/37,669	2.55	OM	AB646440
4512	*atpA*	FoF_1 ATP synthase α subunit	55.2	5.22	13,446/14,894	0.90	IM	AB284111
3401	*atpD*	FoF_1 ATP synthase β subunit	49.9	4.67	14,231/12,568	1.14	IM	AB646451
1505	*cirA*	TonB-dependent receptor	71.9	4.24	8,393/9,412	0.89	OM	AB373987
Group 3. Cell division and morphogenesis								
3308	*mreB*	Cell shape determining protein	37.3	4.96	14,148/5,729	2.47	IM	AB646452
5306	*dacC*	Serine-type D-Ala-D-Ala carboxypeptidase	31.1	6.70	12,684/9,015	1.41	IM	AB646453
3604	*ftsY*	Signal recognition particle-docking protein	61.3	4.69	5,366/2,639	2.03	IM	AB646454
Group 4. Metabolism								
3306	*sliv_c044009*	Transketolase, central region	35.2	4.99	3,716/2,588	1.44	CY	AB646455
3603	*ppsE*	Phosphoenolpyruvate synthase	88.7	4.76	1,369/1,302	1.05	CY	AB646456
7506	*guaB*	Inosine 5'-monophosphate dehydrogenase	51.9	6.77	5,504/2,975	1.85	CY	AB646457
8403	*pykF*	Pyruvate kinase	51.3	5.58	5,454/1,851	2.95	CY	AB646458

Table 2 continued

Spot #	Gene	Protein[a]	Molecular mass (kDa)[b]	p*I*[b]	Spot intensity (ppm) 4°C/18°C	Relative abundance (4°C/18°C)	Predicted localization[c]	Accession no.
6401	*nqrA*	Na^+-translocating NADH-quinone reductase subunit A	47.7	6.06	13,695/15,045	0.91	IM	AB646459
5507	*lpd*	Dihydrolipoamide dehydrogenase	50.7	5.57	5,034/4,678	1.08	IM	AB646460
5601	*aceE*	Pyruvate dehydrogenase subunit	99.3	5.41	6,130/3,988	1.54	CY	AB284092
5412	*ald*	Alanine dehydrogenase	40.0	5.73	8,951/3,504	2.55	IM	AB646461
5303	*leuB*	Isocitrate dehydrogenase	36.2	5.41	6,466/2,676	2.42	CY	AB646462
4511	*sdhA*	Succinate dehydrogenase/fumarate reductase	39.9	5.39	17,451/8,096	2.16	IM	AB646463
7105	*sdhB*	Succinate dehydrogenase iron-sulfur subunit	26.6	6.79	12,273/6,222	1.97	IM	AB646464
4403	*sucB*	Dihydrolipoamide acyltransferase	36.2	5.02	509/184	2.77	CY	AB646465
4311	*sucC*	Succinyl-CoA synthetase β subunit	41.2	5.37	1,184/1,564	0.76	IM	AB646466
5301	*cobB*	NAD-dependent deacetylase	26.7	5.82	4,289/3,981	1.08	CY	AB646467
4208	*ribP_PPkin*	Ribose-phosphate pyrophosphokinase	26.9	5.65	5,614/2,405	2.33	CY	AB646468
3110	*ribH*	Riboflavin synthase	101.9	8.37	15,098/14,919	1.01	CY	AB646475
4602	*pnp*	Polynucleotide phosphorylase/polyadenylase	75.5	5.11	15,780/10,443	1.51	IM	AB646469
5607	*gldC*	Glycine dehydrogenase	104.8	5.70	612/421	1.45	CY	AB646470
3515	*glnA*	Glutamine synthetase	51.9	5.07	9,180/4,903	1.87	CY	AB646471
Group 5. Other functions								
5410	*atoS*	Methyl-accepting chemotaxis sensory transducer PAS domain	48.8	5.96	4,819/<30	>161	IM	AB646472
3301	*rpoA*	DNA-directed RNA polymerase α subunit	36.1	4.64	10,817/10,097	1.07	CY	AB284093
4705	*sliv_c244002*	Peptidase S41	121.4	5.49	2,416/1,386	1.74	CY	AB646473
Group 6. Unknown function								
2203	*sliv_c028017*	Hypothetical protein	28.9	4.66	21,878/17,885	1.22	PE	AB646443
3305	*sliv_c265039*	Hypothetical protein	39.0	4.87	3,163/3,638	0.87	IM	AB646474
2502	*sliv_c361036*	Hypothetical protein	43.5	4.62	8,802/10,344	0.85	IM	AB646444

[a] Proteins in the database showing the highest sequence similarity to the proteins from *S. livingstonensis* Ac10

[b] Molecular mass and p*I* values were calculated using the draft genome sequence of *S. livingstonensis* Ac10

[c] Predicted localizations are characterized as follows: *OM* outer membrane, *PE* periplasm, *IM* inner membrane, *CY* cytoplasm

[d] Two spots for SurA were found in the gel probably due to modification of the protein

grown at temperatures of 4 and 18°C and obtained phospholipid-enriched fractions (Fig. 2). By 2DE analysis of the fraction obtained from the cells grown at 4°C, we detected 276 protein spots with intensity above 500 ppm (Fig. 3a). This number was much higher than that of the crude membrane fraction (180 spots (>500 ppm), Fig. 1), probably as a result of the removal of abundant outer membrane proteins.

Using PMF analysis, we identified 52 proteins in the phospholipid-enriched fractions and found that the predicted subcellular localization of 19 of them was inner membrane (Table 2). The number of predicted outer membrane proteins was 6. In the bottom fraction of the sucrose gradient, we identified predicted outer membrane proteins (OmpA, YaeT, OmpC, TolC2, Sliv_c417088, and CirA), but we obtained no identifiable spot of predicted inner membrane protein in the 2DE gel, even when a larger amount of proteins (450 μg, the maximum loading capacity of the gel) from the bottom fraction was applied to the gel (data not shown). Therefore, the inner membrane was enriched in the middle of the sucrose gradient and separated from the outer membrane (Fig. 2). The sucrose density of the inner membrane-enriched fraction was higher for the cells grown at 4°C than at 18°C, suggesting that the growth temperature affects the composition of proteins and phospholipids of the inner membrane. The ratio of proteins to phospholipids in the inner membrane is probably higher at 4°C than at 18°C, and this may cause the higher membrane density at 4°C.

Proteins with predicted subcellular localization to the periplasm, cytoplasm, and outer membrane were found in the inner membrane-enriched fractions (Table 2). These proteins were recovered in these fractions possibly because of specific and biologically relevant interactions with proteins and phospholipids in the inner membrane. The inner membrane could be the final destination for some of these proteins, where they play physiological roles. We also speculate that some of these periplasmic and outer membrane proteins may be trapped in the inner membrane on route to their final destination by being associated to the translocation apparatus. This could be caused by low translocation efficiency at low temperatures and/or production of a large excess amount of periplasmic and outer membrane proteins. In the future studies, their binding partners in the inner membrane should be analyzed.

We found that the following proteins were more numerous (>2-fold) at 4°C than at 18°C: AtoS, PspA, MreB, FtsY, Ald, SdhA, DegP, SurA, Dpp4, PykF, LeuB, SucB, RibP_PPkin, and Sliv_c417088. These proteins might contribute to protein folding, morphogenesis, sensing the environment, and other cellular processes at low temperatures as discussed in more detail below.

Cold-inducible proteins involved in sensing the environment

The expression of AtoS, the membrane sensor kinase of the AtoSC two-component system, was induced at 4°C (more than 161-fold increase compared with the amount at 18°C). AtoS is a member of the family of Per-ARNT-Sim (PAS) domain-containing proteins, which are important signaling modules that monitor changes in light, redox potential, oxygen, small ligands, and overall energy level of a cell (Taylor and Zhulin 1999). AtoSC has been proposed to participate in many cellular processes, including flagella synthesis and chemotaxis in *E. coli* (Theodorou et al. 2011). We previously found that the cell motility of *S. livingstonensis* Ac10 at 4°C was more notable than at 18°C, and that the production of the flagella-related proteins FlgE and FlgL was increased at 4°C compared to that at 18°C. AtoS may be involved in the inducible production of these flagella-related proteins and thereby contribute to the increased motility of this bacterium at low temperatures. The diffusion rate of nutrient compounds is decreased at low temperatures as a result of the low diffusion coefficient and high water viscosity compared to moderate temperatures. Under such unfavorable conditions, the bacterium might show increased motility to facilitate movement towards more favorable environments.

Cold-inducible proteins involved in biogenesis of membrane proteins

We found that the periplasmic chaperones DegP (also known as HtrA) and SurA are expressed at low temperatures. These proteins are located adjacent to the membrane phospholipids and/or inner membrane secretion systems, such as the Sec apparatus (de Keyzer et al. 2003; Sklar et al. 2007), and are involved in the targeting pathway of outer membrane integral β-barrel proteins (Ruiz et al. 2006). We previously reported that 2 putative outer membrane porin homologs, OmpA and OmpC, are inducibly expressed at 4°C, which may counteract the low diffusion rate of solutes at low temperatures and enable the efficient uptake of nutrients (Kawamoto et al. 2007). Cold-inducible periplasmic chaperones, DegP and SurA, are thought to be important for increased production of these membrane proteins at low temperatures because low thermal energy and high aqueous viscosity at low temperatures may decrease the efficiency of protein folding.

The bacterial signal recognition particle (SRP) receptor FtsY was also inducibly expressed at low temperatures. FtsY plays a key role in membrane protein targeting and provides the essential link between the soluble SRP-ribosome-nascent chain complexes and the membrane-bound Sec translocon (Koch et al. 2003). FtsY interacts with the

SRP protein Ffh (Parlitz et al. 2007) and induces GTP-dependent dissociation of SRP from the nascent-peptide chain. Cold induction of FtsY suggests that it plays a role in dissociation of membrane protein precursors from SRP to facilitate production of membrane proteins at low temperatures.

Cold-inducible proteins involved in morphogenesis

We identified an actin-like cytoskeleton protein, MreB, as a cold-inducible protein. In bacteria, the process of cell elongation is controlled by MreB, which is believed to localize components of the peptidoglycan synthetic machinery along the lateral cell wall, thereby governing the geometry of cell wall growth (Varma and Young 2009; Vats et al. 2009). Thus, MreB is possibly involved in morphogenesis of *S. livingstonensis* Ac10 at low temperatures. We previously found that this bacterium shows morphological changes in response to its growth temperature: the cells were significantly shorter at 4°C than at 18°C. MreB may play a role in regulating the morphology of *S. livingstonensis* Ac10 at low temperatures.

Conclusions

We previously identified proteins inducibly produced at low temperatures in *S. livingstonensis* Ac10, which suggests that proteins involved in various cellular processes, such as gene expression, protein synthesis and folding, membrane transport, motility, and cell division, support its growth at low temperatures (Kawamoto et al. 2007). Recent proteomic studies also identified a lot of cold-inducible proteins and illustrate how cellular processes of cold-adapted bacteria proceed at low temperatures (Ting et al. 2010; Piette et al. 2011; Wilmes et al. 2011). Nevertheless, there is little information about their inner membrane, which is involved in primary cellular processes of Gram-negative bacteria, such as respiration, membrane transport, and cell division. The present work represents the first attempt to separate outer and inner membranes of a psychrotrophic bacterium and provides new clues to elucidate the cold-adaptation mechanism of *S. livingstonensis* Ac10. Although the physiological roles of cold-inducible inner membrane proteins remain unclear, further characterization of these proteins may be helpful to understand the mechanism of cellular adaptation to cold environments.

Acknowledgments This work was supported in part by the Grants-in-Aid for Scientific Research (B) from JSPS (20360372 and 22404021 to T.K. and 21405038 to J.K.), Grant-in-Aid for Challenging Exploratory Research 22658028 (to T.K.), a Grant from the Institute for Fermentation, Osaka (to T.K.), a Grant from Japan Foundation for Applied Enzymology (to T.K.), the grant for Research for Promoting Technological Seeds 10-041 from JST (to J.K.), and a Global COE program Integrated Materials Science (to J.K.).

References

Bligh EG, Dyer WJ (1959) A rapid method of total lipid extraction and purification. Can J Biochem Physiol 37:911–917

Chintalapati S, Kiran MD, Shivaji S (2004) Role of membrane lipid fatty acids in cold adaptation. Cell Mol Biol (Noisy-le-grand) 50:631–642

de Keyzer J, van der Does C, Driessen AJ (2003) The bacterial translocase: a dynamic protein channel complex. Cell Mol Life Sci 60:2034–2052

Feller G, Gerday C (2003) Psychrophilic enzymes: Hot topics in cold adaptation. Nat Rev Microbiol 1:200–208

Hebraud M, Potier P (1999) Cold shock response and low temperature adaptation in psychrotrophic bacteria. J Mol Microbiol Biotechnol 1:211–219

Kawamoto J, Kurihara T, Kitagawa M, Kato I, Esaki N (2007) Proteomic studies of an antarctic cold-adapted bacterium, *Shewanella livingstonensis* Ac10, for global identification of cold-inducible proteins. Extremophiles 11:819–826

Koch HG, Moser M, Muller M (2003) Signal recognition particle-dependent protein targeting, universal to all kingdoms of life. Rev Physiol Biochem Pharmacol 146:55–94

Koenig T, Menze BH, Kirchner M, Monigatti F, Parker KC, Patterson T, Steen JJ, Hamprecht FA, Steen H (2008) Robust prediction of the mascot score for an improved quality assessment in mass spectrometric proteomics. J Proteome Res 7:3708–3717

Kulakova L, Galkin A, Kurihara T, Yoshimura T, Esaki N (1999) Cold-active serine alkaline protease from the psychrotrophic bacterium *Shewanella* strain Ac10: gene cloning and enzyme purification and characterization. Appl Environ Microbiol 65:611–617

Mineki R, Taka H, Fujimura T, Kikkawa M, Shindo N, Murayama K (2002) In situ alkylation with acrylamide for identification of cysteinyl residues in proteins during one- and two-dimensional sodium dodecyl sulphate-polyacrylamide gel electrophoresis. Proteomics 2:1672–1681

Murray RG, Steed P, Elson HE (1965) The location of the mucopeptide in sections of the cell wall of *Escherichia coli* and other Gram-negative bacteria. Can J Microbiol 11:547–560

Osborn MJ, Munson R (1974) Separation of the inner (cytoplasmic) and outer membranes of Gram-negative bacteria. Methods Enzymol 31:642–653

Parlitz R, Eitan A, Stjepanovic G, Bahari L, Bange G, Bibi E, Sinning I (2007) *Escherichia coli* signal recognition particle receptor FtsY contains an essential and autonomous membrane-binding amphipathic helix. J Biol Chem 282:32176–32184

Piette F, D'Amico S, Mazzucchelli G, Danchin A, Leprince P, Feller G (2011) Life in the cold: a proteomic study of cold-repressed proteins in the antarctic bacterium *Pseudoalteromonas haloplanktis* TAC125. Appl Environ Microbiol 77:3881–3883

Rouser G, Siakotos AN, Fleischer S (1966) Quantitative analysis of phospholipids by thin-layer chromatography and phosphorus analysis of spots. Lipids 1:85–86

Ruiz N, Kahne D, Silhavy TJ (2006) Advances in understanding bacterial outer-membrane biogenesis. Nat Rev Microbiol 4:57–66

Russell NJ (1997) Psychrophilic bacteria—molecular adaptations of membrane lipids. Comp Biochem Physiol A Physiol 118:489–493

Siddiqui KS, Cavicchioli R (2006) Cold-adapted enzymes. Annu Rev Biochem 75:403–433

Sklar JG, Wu T, Kahne D, Silhavy TJ (2007) Defining the roles of the periplasmic chaperones SurA, Skp, and DegP in *Escherichia coli*. Genes Dev 21:2473–2484

Taylor BL, Zhulin IB (1999) PAS domains: internal sensors of oxygen, redox potential, and light. Microbiol Mol Biol Rev 63:479–506

Theodorou EC, Theodorou MC, Kyriakidis DA (2011) Inhibition of the signal transduction through the AtoSC system by histidine kinase inhibitors in *Escherichia coli*. Cell Signal 23:1327–1337

Ting L, Williams TJ, Cowley MJ, Lauro FM, Guilhaus M, Raftery MJ, Cavicchioli R (2010) Cold adaptation in the marine bacterium, *Sphingopyxis alaskensis*, assessed using quantitative proteomics. Environ Microbiol 12:2658–2676

Varma A, Young KD (2009) In *Escherichia coli*, MreB and FtsZ direct the synthesis of lateral cell wall via independent pathways that require PBP 2. J Bacteriol 191:3526–3533

Vats P, Yu J, Rothfield L (2009) The dynamic nature of the bacterial cytoskeleton. Cell Mol Life Sci 66:3353–3362

Wilmes B, Kock H, Glagla S, Albrecht D, Voigt B, Markert S, Gardebrecht A, Bode R, Danchin A, Feller G, Hecker M, Schweder T (2011) Cytoplasmic and periplasmic proteomic signatures of exponentially growing cells of the psychrophilic bacterium *Pseudoalteromonas haloplanktis* TAC125. Appl Environ Microbiol 77:1276–1283

Yamanaka K, Fang L, Inouye M (1998) The CspA family in *Escherichia coli*: multiple gene duplication for stress adaptation. Mol Microbiol 27:247–255

Yamato I, Anraku Y, Hirosawa K (1975) Cytoplasmic membrane vesicles of *Escherichia coli*. A simple method for preparing the cytoplasmic and outer membranes. J Biochem 77:705–718